Dynamic structure factor for the Fibonacci-chain quasicrystal

J. A. Ashraff and R. B. Stinchcombe
Department of Theoretical Physics, Oxford University, 1 Keble Road, Oxford, OX1 3NP, United Kingdom
(Received 17 February 1988)

We have performed an exact real-space renormalization-group calculation of the complete wave-vector- and frequency-dependent-response function, $S(q,\omega)$, for the one-dimensional Fibonacci-chain quasicrystal with "Goldstone" dynamics as in the case of phonons or magnons. We present surface plots, which are highly structured, of the full response $S(q,\omega)$, for different values of the coupling ratio. In addition, we have obtained a hierarchy of dispersion curves of ω versus q which contain features related to the gap structure of the excitation spectrum. The limiting case of equal couplings, while still nontrivial because of geometric effects, is analytically tractable and gives a useful test of the renormalization-group treatment, of which it is a special case, and when extended using degenerate perturbation theory it provides an interpretation of the general situation.

I. INTRODUCTION

Quasiperiodic systems in one dimension are currently receiving considerable attention. Although various properties of the spectra have been studied in the past,[1-3] it was not until the discovery of a quasicrystalline phase of AlMn by Shechtman *et al.*[4] and the subsequent interpretation by Levine and Steinhardt[5] in terms of the aperiodic but space filling Penrose lattice (of which the Fibonacci chain is the one-dimensional realization), that such activity has intensified.

Until recently all the results concerning the mathematical and physical properties of the Fibonacci chain have been obtained using the transfer matrix approach introduced independently by Kohmoto, Kadanoff, and Tang[2] and by Ostlund and Pandit.[3] This method involves using the Fibonacci inflation rule

$$A_n \rightarrow A_{n+1}B_{n+1}\,, \tag{1.1a}$$

$$B_n \rightarrow A_{n+1} \tag{1.1b}$$

to construct the following third order difference equation for $\gamma_n = \frac{1}{2}\mathrm{Tr}(\mathbf{T_n})$, where $\mathbf{T_n}$ is the dynamic transfer matrix describing level n of the hierarchy

$$\gamma_{n+1} = 2\gamma_n\gamma_{n-1} - \gamma_{n-2}\,. \tag{1.2}$$

The electronic (or phonon) spectrum is then obtained by iterating (1.2) from three initial values γ_{-1}, γ_0, and γ_1 which are known functions of energy E (or squared frequency ω^2) and the remaining system parameters, and examining the asymptotic behavior of the γ_n's.[2]

It is now accepted that the spectrum is a Cantor set of zero Lebesgue measure corresponding to critical eigenfunctions[6] (i.e., neither extended nor localized). In addition, the quantity

$$I = \gamma_{n+1}^2 + \gamma_n^2 + \gamma_{n-1}^2 - 2\gamma_{n+1}\gamma_n\gamma_{n-1} - 1 \tag{1.3}$$

was shown by Kohmoto *et al.* to remain invariant under the action of (1.2) and is therefore (from its value at $n=0$) a known function of energy (or ω^2). It was also shown by Kohmoto *et al.* that for a specific tight binding electronic model the exponents describing the scaling of the spectrum near the upper band edge and band center ($E=0$) were governed by 2 and 6 cycles of the form

$$\alpha \rightarrow \beta \rightarrow \alpha \rightarrow \ldots \tag{1.4}$$

and

$$\alpha \rightarrow 0 \rightarrow 0 \rightarrow -\alpha \rightarrow 0 \rightarrow 0 \rightarrow \alpha \rightarrow \ldots\,, \tag{1.5}$$

respectively. Furthermore, Luck and Nieuwenhuizen[7] later found another six cycle of the form

$$\alpha \rightarrow -\beta \rightarrow -\alpha \rightarrow \beta \rightarrow -\alpha \rightarrow \beta \rightarrow \alpha \rightarrow \ldots \tag{1.6}$$

of which (1.5) is a special case, and later, in collaboration with Petritis, Luck showed[8] that the scaling properties of the upper edge of the phonon spectrum is governed by (1.6). Finally, by linearizing about the two and six-cycle fixed points one can obtain exponents which, through the invariant (1.3), can be related to the energy E (or squared frequency ω^2). Indeed, every gap edge in the spectrum (of which there are infinitely many) is associated with its own scaling exponent. The $f(\alpha)$ curve characterizing such multifractal aspects has been discussed by Kohmoto *et al.*,[6] by Evangelou[9] and more recently by Hawrylak *et al.*[10] in the context of the Fibonacci superlattice.

It has been known for some time how to use real space renormalization group techniques (especially decimation) to obtain standard dynamic scaling properties (exponents, etc.) for linear dynamical processes at a continuous phase transition, or on self-similar backgrounds (nonrandom[11] and random fractals[12]). A particularly powerful implementation of the technique is that using a generating function to obtain the density of states[13,14] and the full wave vector and frequency dependent response function.[15] Also, such methods are not restricted to one dimension and can be applied to regular[16] and nonuniform fractal[13,15] lattices in two and higher dimensions, which is not possible with the transfer matrix approach. With such extensions in mind it has been considered of some importance to develop corresponding decimation tech-

niques for quasicrystals. This was initially done by Lu *et al.*[17] who combined a continued fraction expansion together with a decimation transformation, to show that both the electronic and phonon spectra of the Fibonacci chain quasicrystal were Cantor-like. More recently, Kantha and Stinchcombe have applied decimation techniques to the problem of diffusion on the Fibonacci chain and have obtained the exponent characterizing the long time dynamics.[18] In a previous paper,[19] an exact decimation procedure was developed for the one-dimensional Fibonacci chain quasicrystal, providing an *a priori* exact determination of all the dynamic quantities, including the full Green functions G_{ij}. The decimation procedure does not rely on any translational invariance and exploits in a very direct way the hierarchical properties of the quasicrystal. The associated rescaling transformation yields not only information on exponents via a fixed point (or cycle) analysis, but also provides an efficient computational means of obtaining the spectrum (density of states). The density of electronic states, $\rho(E)$, for a system of tight binding electrons [or $\rho(\omega^2)$ for a phonon system], which is related to the imaginary part of the diagonal Green function, was calculated, and our results led us to conjecture that the scaling properties of all gap edges within the spectrum were governed by the general six cycle (1.6). In addition we found that ln-ln plots of the density of states against energy E (or ω^2) near a gap edge were periodic with period related to the exponent describing the scaling of the spectrum at the same gap edge.

It should be noted that physical realizations of the Fibonacci chain quasicrystal do in fact exist. Merlin *et al.*[20] were the first to succeed in growing a quasiperiodic superlattice, consisting of alternating layers of GaAs and AlAs corresponding to 13 generations (iterations) of the rule (1.1). The Raman scattering measurements they have carried out led to a spectrum with dips at certain values of ω which they ascribed to the gaps in the density of states spectrum. More recently, both experimental and theoretical studies of Raman scattering from acoustic phonons in Si-Ge_xSi_{1-x} strained-layer Fibonacci superlattices[21] and the plasmon spectrum of an array of two-dimensional electron-gas layers arranged in a Fibonacci sequence[10] have been reported.

In the present paper we present, for the first time, a calculation of the complete wave vector and frequency-dependent response function (dynamic structure factor) $S(q,\omega)$, for a Fibonacci chain with spin wave or phonon dynamics. Such a quantity is related to the cross section obtained in an inelastic neutron scattering experiment[22] and so is clearly of importance. We shall assume that the spins (or atoms in the phonon case) reside on a lattice $\mathcal{L}$ of sites such that

$$d_{ij}=\begin{cases} d_A, \\ d_B , \end{cases} \tag{1.7}$$

according to the rule (1.1) where d_{ij} denotes the distance between a nearest-neighbor pair of sites i and j.

Our method of calculation is based upon the previously mentioned real space renormalization-group approach, and is a generalization of the techniques introduced by Tremblay and Southern[13] for the density of states and by Maggs and Stinchcombe[15] for the complete q and ω dependent response function. The associated recursive evaluation of the full Green function $G(q,\omega)$ is given in Sec. 2. Subsequent sections contain detailed numerical results, including surface plots of $S(q,\omega)$ (Sec. III), and an interpretation via a soluble but characteristic "equal coupling" limit and its perturbation theory extension (Sec. IV); Sec. V is a concluding discussion.

II. THE DYNAMIC STRUCTURE FACTOR: A GENERATING FUNCTION APPROACH

Although the techniques and results to be presented in this paper are of a general nature and apply to any dynamic process obeying a linear equation of motion and possessing a Goldstone symmetry, to be specific we shall consider the case of Heisenberg ferromagnetic spin waves on the Fibonacci chain; the replacement $\omega\rightarrow\omega^2$ and exchange constants by spring constants provides corresponding results for lattice vibrations, etc.

The dynamic structure factor $S(q,\omega)$ is given by

$$S(q,\omega)=\lim_{\eta\rightarrow 0}\lim_{N\rightarrow\infty}\mathrm{Im}G_N(q,\omega-i\eta) , \tag{2.1}$$

where

$$G_N(q,\omega)=\frac{1}{N}\sum_{l,l'} e^{iq(r_l-r_{l'})}G_{ll'}(\omega) , \tag{2.2}$$

r_l denoting the position of site l on the lattice $\mathcal{L}$ and N the number of sites. The Green functions G_{ij} satisfy the following linear equation of motion

$$(L_i-\omega)G_{ij}=\delta_{ij}+\sum_k J_{ik}G_{kj} , \tag{2.3}$$

where $L_i=\sum_k J_{ik}$, k denoting a nearest-neighbor site of i. Introducing the $N\times N$ matrix $\mathbf{H}$ having elements

$$H_{ii}=L_i-\omega , \tag{2.4a}$$

$$H_{ij}=-J_{ij} , \tag{2.4b}$$

it follows that (2.3) can be written in matrix form as

$$\mathbf{HG}=\mathbf{I} , \tag{2.5}$$

where $\mathbf{G}$ is a matrix whose elements are precisely G_{ij} as in (2.3) and $\mathbf{I}$ is the identity matrix.

The calculation of the G_{ij} is facilitated by introducing the generating function

$$\mathcal{F}_N\{b\}=\ln\Xi_N\{b\} , \tag{2.6}$$

where $\{b\}$ denotes a set of (site dependent) generic fields and

$$\Xi_N\{b\}=\int\mathcal{D}\mathcal{S}\exp\left[\frac{i\mathcal{A}}{2}\right] , \tag{2.7a}$$

$$\int\mathcal{D}\mathcal{S}=\prod_{i=1}^{N}\int_{-\infty}^{+\infty}dS_i , \tag{2.7b}$$

with

$$\mathcal{A}=\mathbf{S}^T\mathbf{H}\mathbf{S}+2\mathbf{b}^T\mathbf{S}$$
$$=\sum_i (L_i-\omega)S_i^2-\sum_{ij} J_{ij}S_iS_j+2\sum_i b_iS_i \ . \tag{2.8}$$

A formal evaluation of the Gaussian integrals appearing in (2.6) leads to the result

$$\mathcal{F}\{b\}=-\tfrac{1}{2}i\sum_{ij} b_iG_{ij}b_j \ , \tag{2.9}$$

where we have ignored a field independent constant. It thus follows that

$$G_{ij}=i\frac{\partial^2}{\partial b_i\partial b_j}\mathcal{F}\{b\} \tag{2.10}$$

and so in terms of $\mathcal{F}$ we can write (2.2) as

$$G_N(q,\omega)=\frac{i}{N}\sum_{ll'} e^{iq(r_l-r_{l'})}\frac{\partial^2}{\partial b_l\partial b_{l'}}\mathcal{F}_N\{b\} \ . \tag{2.11}$$

Now, in the spirit of the renormalization group we shall calculate $\mathcal{F}\{b\}$ recursively by successively performing a fraction of the integrals appearing in (2.7). In order to implement that, it is convenient to partition the lattice $\mathcal{L}$ into two sublattices which we shall denote by $\mathcal{L}_1$ and $\mathcal{L}_2$, corresponding to the sublattice of sites which remain and are to be eliminated, respectively. Then in terms of these sublattice variables, our previous expression (2.8) can be written

$$\mathcal{A}(b)=\mathbf{S}_1^T\mathbf{H}_{11}\mathbf{S}_1+\mathbf{S}_1^T\mathbf{H}_{12}\mathbf{S}_2+\mathbf{S}_2^T\mathbf{H}_{21}\mathbf{S}_1$$
$$+\mathbf{S}_2^T\mathbf{H}_{22}\mathbf{S}_2+2\mathbf{b}_1^T\mathbf{S}_1+2\mathbf{b}_2^T\mathbf{S}_2 \ . \tag{2.12}$$

Performing the Gaussian integrals over the variables associated with the sublattice $\mathcal{L}_2$ and a site relabeling, we obtain a decimated action of the form

$$\mathcal{A}(b')=\mathbf{S}^T\mathbf{H}'\mathbf{S}+2\mathbf{b}'^T\mathbf{S} \ , \tag{2.13}$$

where

$$\mathbf{H}'=\mathbf{H}_{11}-\mathbf{H}_{12}\mathbf{H}_{22}^{-1}\mathbf{H}_{21} \ , \tag{2.14a}$$

$$\mathbf{b}'=\mathbf{b}_1-\mathbf{H}_{12}\mathbf{H}_{22}^{-1}\mathbf{b}_2 \ . \tag{2.14b}$$

Now, under this same transformation by scaling factor $\tilde{b}$, $\mathcal{F}$ scales like

$$\mathcal{F}_N\{b,\omega\}=C(b,\omega)+\mathcal{F}_{N'}\{b',\omega\} \ , \tag{2.15}$$

where $N'=N/\tilde{b}$ and for fixed b and ω, C is a constant arising from the completion of the square in carrying out the Gaussian integration and obeys the following recursion relation:

$$C'=C+\frac{i}{2}\mathbf{b}_2^T\mathbf{H}_{22}^{-1}\mathbf{b}_2 \ . \tag{2.16}$$

It should be noted that the renormalization group ideas leading to (2.16) are analogous to those which have been used in the past in the context of thermal critical phenomena,[23] and indeed the result (2.15) is very similar to that which one would obtain for the scaling of the usual free energy in a thermal problem. Defining the contribution of such a constant term (2.16) to (2.11) at the nth stage of such an elimination process by $I_N^{(n)}(q,\omega)$, it follows from (2.16) that

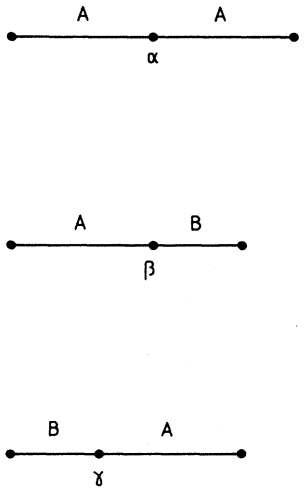

FIG. 1. The three distinct types of sites.

$$I_N^{(n)}(q,\omega)=-\frac{1}{2N}\sum_{ll'mm'} e^{iq(r_l-r_{l'})}\frac{\partial^2}{\partial b_m\partial b_{m'}}$$
$$\times(\mathbf{b}_2^T)_m^{(n-1)}(\mathbf{H}_{22}^{-1})_{mm'}^{(n-1)}(\mathbf{b}_2)_{m'}^{(n-1)} \ , \tag{2.17}$$

where all derivatives are implicitly assumed to be with respect to the zeroth-order fields $\{b^{(0)}\}$. Whereas the discussion from (2.9) to (2.17) applies to any one-dimensional lattice, the procedure is only tractable for the Fibonacci chain with a very special choice of sites to decimate. In Fig. 1 we have shown the three different types of sites for the Fibonacci lattice and in Fig. 2 we illustrate the decimation for a chain containing F_5 sites, where it is clear that only sites of the type β are eliminated. It is thus necessary to distinguish between the six different types of site terms appearing in (2.8) and so we define

$$L_i=\begin{cases} L_\alpha & \text{if } i\in\mathcal{L}_\alpha \ , \\ L_\beta & \text{if } i\in\mathcal{L}_\beta \ , \\ L_\gamma & \text{if } i\in\mathcal{L}_\gamma \ , \end{cases} \tag{2.18a}$$

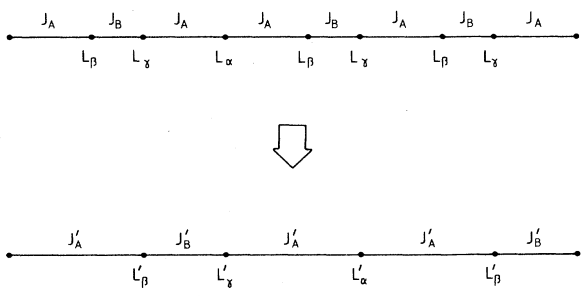

FIG. 2. The decimation procedure illustrated for a chain of 9 sites.

and

$$b_i=\begin{cases} f_i & \text{if } i\in\mathcal{L}_\alpha\ , \\ g_i & \text{if } i\in\mathcal{L}_\beta\ , \\ h_i & \text{if } i\in\mathcal{L}_\gamma\ , \end{cases} \tag{2.18b}$$

where $\mathcal{L}_\alpha$, $\mathcal{L}_\beta$, and $\mathcal{L}_\gamma$ denote sublattices of type α, β, and γ, respectively, with $\mathcal{L}=\mathcal{L}_\alpha\cup\mathcal{L}_\beta\cup\mathcal{L}_\gamma$. Furthermore, we define our exchange constants J_{ij} such that J_A and J_B correspond to the exchange interactions between two nearest-neighbor sites separated by distances d_A and d_B, respectively.

For the particular case of the Fibonacci chain with F_N sites we have the result

$$(\mathbf{H}_{22}^{-1})^{(n)}_{mm'}=(L_\beta^{(n)}-\omega)^{-1}\delta_{mm'}\ , \tag{2.19}$$

which applies because only sites of type β are eliminated and such sites are never nearest neighbors of each other, and so it follows that

$$I_{F_N}^{(n)}(q,\omega)=-\frac{1}{2F_N(L_\beta^{(n-1)}-\omega)} \times\sum_{ll'm} e^{iq(r_l-r_{l'})}\frac{\partial^2}{\partial b_l\partial b_{l'}}g_m^{(n-1)}g_m^{(n-1)}\ , \tag{2.20}$$

where $g_m^{(n)}$ denotes the nth iterate of the zeroth-order field $g_m^{(0)}$ under the renormalization group transformation. Now, for general n the nth order fields $g_m^{(n)}$ are complicated functions of the zeroth-order fields $\{b^{(0)}\}$ and we write

$$g_m^{(n)}=\sum_r X_{m,r}^{(n)}b_r^{(0)}\ . \tag{2.21}$$

Thus (2.20) becomes

$$I_{F_N}^{(n)}(q,\omega)=-\frac{1}{F_N}\frac{1}{(L_\beta^{(n-1)}-\omega)} \times\sum_{ll'm} e^{iq(r_l-r_{l'})}X_{m,l}^{(n-1)}X_{m,l'}^{(n-1)}\ . \tag{2.22}$$

Then, Fourier transforming (2.21) and taking unit amplitudes for the field acting on the original lattice allows us to write (2.22) as

$$I_N^{(n)}(q,\omega)=-\frac{F_{N-2}}{F_N}\frac{1}{(L_\beta^{(n-1)}-\omega)}\tilde{g}_q^{(n-1)}\tilde{g}_{-q}^{(n-1)}\ . \tag{2.23}$$

Letting $N\to\infty$ we obtain

$$I^{(n)}(q,\omega)=-\frac{1}{\tau^{n+1}}\frac{1}{(L_\beta^{(n-1)}-\omega)}\tilde{g}_q^{(n-1)}\tilde{g}_{-q}^{(n-1)}\ . \tag{2.24}$$

Finally, the full Green function $G(q,\omega)$ is given by

$$G(q,\omega)=\sum_{n=1}^{\infty} I^{(n)}(q,\omega)\ . \tag{2.25}$$

The implementation of this scheme is given in the next section.

III. RESULTS

It is clear that in order to carry out the procedure described in the previous section, and in particular to calculate $G(q,\omega)$ using (2.23), that we require a closed set of recursion relations for the parameters appearing in (2.3) as well as for the fields f_i, g_i, and h_i. From (2.14a) we obtain directly using (2.17)

$$\begin{aligned} J_A'&=\frac{J_AJ_B}{L_\beta-\omega}\ , \\ J_B'&=J_A\ , \\ L_\alpha'&=L_\gamma-\frac{J_A^2+J_B^2}{L_\beta-\omega}\ , \\ L_\beta'&=L_\gamma-\frac{J_B^2}{L_\beta-\omega}\ , \\ L_\gamma'&=L_\alpha-\frac{J_A^2}{L_\beta-\omega}\ , \end{aligned} \tag{3.1}$$

and from (2.14b) for the fields we have

$$\begin{aligned} f_i'&=h_i+\frac{J_Bg_{i-1}+J_Ag_{i+1}}{L_\beta-\omega}\ , \\ g_i'&=h_i+\frac{J_Bg_{i-1}}{L_\beta-\omega}\ , \\ h_i'&=f_i+\frac{J_Ag_{i+1}}{L_\beta-\omega}\ . \end{aligned} \tag{3.2}$$

Finally, Fourier transforming the set (3.2) yields the following set of recursion relation for the Fourier components $\tilde{f}_q$, $\tilde{g}_q$, and $\tilde{h}_q$:

$$\begin{aligned} \tilde{f}'_{\tau q}&=\tilde{h}_q+\tilde{g}_q\frac{J_Be^{-iq}-J_Ae^{i\tau q}}{L_\beta-\omega}\ , \\ \tilde{g}'_{\tau q}&=\tilde{g}_q+\tilde{g}_q\frac{J_Be^{-iq}}{L_\beta-\omega}\ , \\ \tilde{h}'_{rq}&=\tilde{f}_q+\tilde{g}_q\frac{J_Ae^{i\tau q}}{L_\beta-\omega}\ . \end{aligned} \tag{3.3}$$

The procedure to generate $G(q,\omega)$ and hence $S(q,\omega)$ [see (2.1)] is thus as follows: starting from a fixed (complex) frequency ω, the physical values of the parameters $(J_A,J_B,L_\alpha=2J_A,\ L_\beta=L_\gamma=J_A+J_B,\ f_i=g_i=h_i=1)$ are transformed according to Eqs. (3.1) and (3.3) and at each successive stage $I^{(n)}$ is evaluated using (2.22) and accumulated as in (2.23).

In Figs. 3 and 4 we have shown surface plots of the resulting $S(q,\omega)$ as functions of both q and ω for $J_B/J_A=1$ and $J_B/J_A=2$. The finite width of the peaks is due to the finite imaginary part η used in the frequency. It should be emphasized however, that η is entirely arbitrary and we have used $\eta=1\times10^{-20}$ without problems. In fact, in physically realizable situations level broaden-

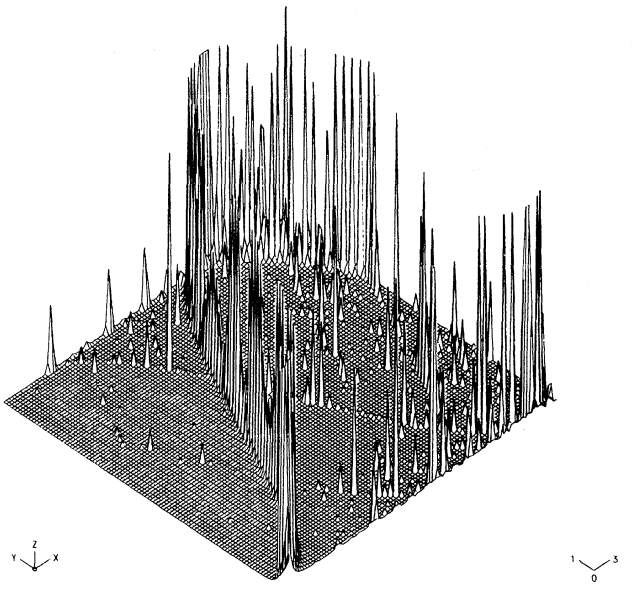

FIG. 3. A surface plot of $S(q,\omega)$ as a function of q/α and ω/J_A for $J_B/J_A=1$. The x axis corresponds to q/α and the y axis to ω/J_A.

ing is likely to occur and for comparison the theory should then include a corresponding imaginary part in the frequency.

Note that in the "pure" limit $J_A=J_B$ shown in Fig. 3 the peaking of the structure factor in the ω,q plane is not confined to the well known dispersion curve $\omega(q)=2(1-\cos q)$ for the usual linear chain consisting of

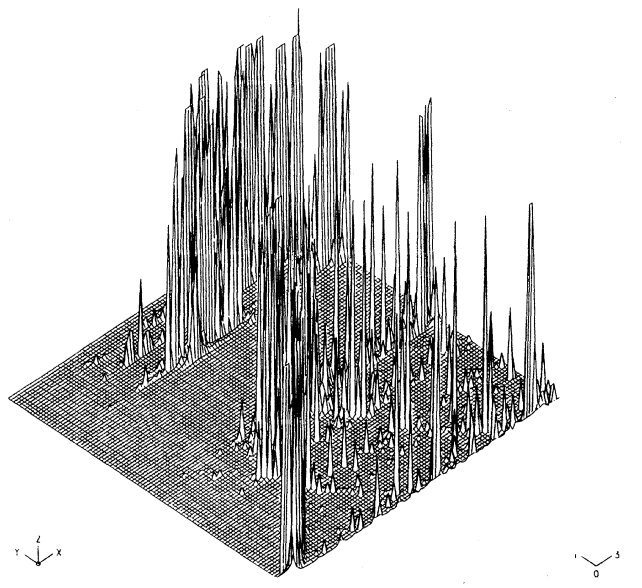

FIG. 4. A surface plot of $S(q,\omega)$ as a function of q/α and ω/J_A for $J_B/J_A=2$. The x axis corresponds to q/α and the y axis to ω/J_A.

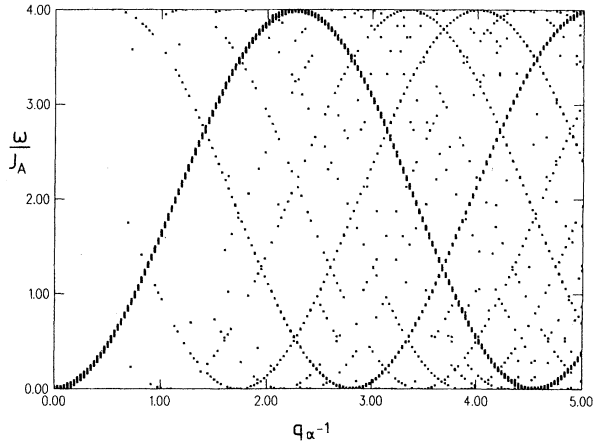

FIG. 5. A plot of ω/J_A vs q/α for $J_B/J_A=1$.

equally spaced sites but instead a curve of the usual type is accompanied by (infinitely) many satellite curves. This is due to the particular geometry arising from the nonuniform tiling and leading to the appearance of nontrivial phase factors in the defining equation (2.2) for $G(q,\omega)$ and in the recursion relations for the fields, leading to the different form for $S(q,\omega)$. This case of equal coupling has however, proved to be analytically tractable and we treat this in the next section where the existence of the satellite peaks and their intensity is explained.

The full response for the nontrivial case of $J_B/J_A=2$ shown in Fig. 4 is clearly of a highly complex nature with gaps appearing at values of ω where the density of states $\rho(\omega)$ is known to be zero.[19] To obtain dispersion curves of ω versus q from the $S(q,\omega)$ data we show in Figs. 5–8 plots of those values of ω and q for which the response $S(q,\omega)\geq 1.0$ for the four cases $J_B/J_A=1$, 1.2, 1.6, and 2, respectively. Figure 5 for the "pure" case ($J_A=J_B$) displays very clearly the prominent S-shaped band reminiscent of the $2(1-\cos q)$ dispersion curve together with

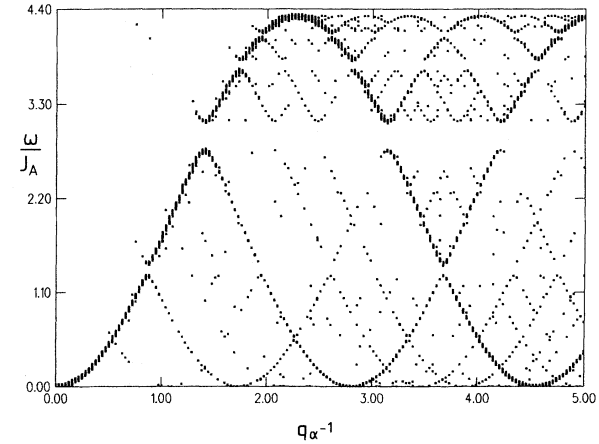

FIG. 6. A plot of ω/J_A vs q/α for $J_B/J_A=1.2$.

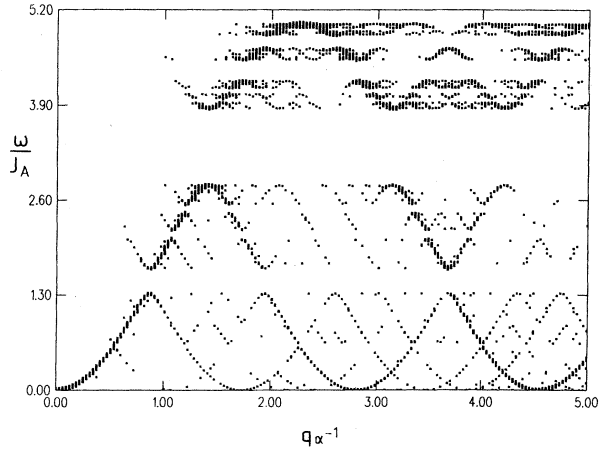

FIG. 7. A plot of ω/J_A vs q/α for $J_B/J_A=1.6$.

additional "satellite" subbands. In addition, the gaps in the excitation spectrum arising in the nontrivial case of $J_B/J_A\neq 1$, lead to a striped aspect as is evident from Figs. 7 and 8. The interpretation of all these features is presented in the next section.

IV. INTERPRETATION; A SOLUBLE LIMIT AND EXTENSIONS

The surface plots of $S(q,\omega)$ indicate that it has a great deal of structure, with most of the intensity coming near certain curves in the $\omega-q$ plane, as is evident from Figs. 5–8. Even in the case of equal couplings (Fig. 5) there is more than one such curve unlike the situation in an equal coupling chain with equal atomic spacings. The Fibonacci chain with equal couplings (but aperiodic atomic spacings) has therefore a nontrivial structure factor, and since it turns out to be exactly soluble it can provide an understanding of the origin of the different curves, as will be shown shortly.

The obvious difference between the equal coupling and the general cases ($J_A=J_B$) is the appearance in Figs. 6–8 of stripes, parallel to the q axis, of zero response. They correspond to gaps in the spectrum i.e., the frequency regions containing no eigenenergies. These gaps occur everywhere so our reference to "curves" of nonzero intensity or response $[S(q,\omega)]$ has to be understood as a loose terminology, when $J_A=J_B$. It will be shown later in this section that the gaps and the associated modification of the "curves" can be at least qualitatively explained by a degenerate perturbation theory extension of the equal coupling limit.

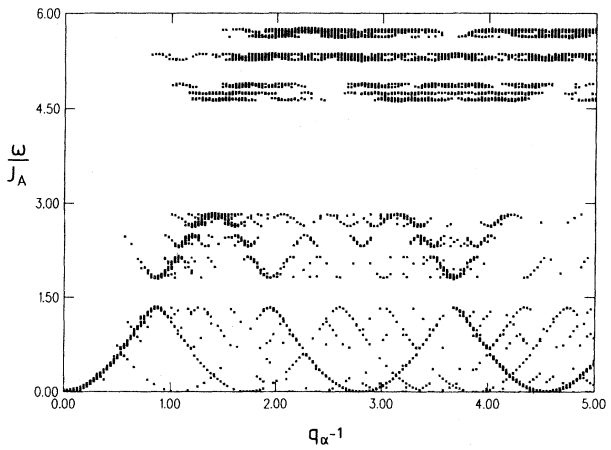

FIG. 8. A plot of ω/J_A vs q/α for $J_B/J_A=2$.

One interesting feature is that the curve through the origin has, especially near the origin, a large intensity. The reason for this is that an excitation of small wave vector q sees the Fibonacci lattice as very like a continuum and is therefore asymptotically an eigenstate for any J_A and J_B. However, for $q\neq 0$ it is not an eigenstate, even in the equal coupling case, and this can already be seen by the fact that a line of fixed q intersects many curves of nonzero $S(q,\omega)$, and this corresponds to the overlap of the wavelike state with many eigenstates.

We now treat the Fibonacci chain with equal couplings ($J_A=J_B$) but still retaining the different tile lengths ($d_A:d_B=\tau:1$). It is obviously crucial to distinguish the site label n from the actual position r_n of the nth site. For, a wavelike excitation periodic in n (i.e., of the form e^{ikn}) is an eigenstate of the equal coupling Fibonacci chains with eigenenergy

$$\omega_k=2J(1-\cos k)\ , \tag{4.1}$$

while the wave e^{iqr_n}, which is the probe for which the dynamic structure factor provides the response, is not an eigenstate. Clearly, by decomposing the probe wave into eigenstates we obtain

$$S(q,\omega)=\sum_{nn'k} e^{[iq(r_n-r_{n'})-i(n-n')k]}\delta(\omega-\omega_k)\ . \tag{4.2}$$

So it is the geometry of the chain, rather than its dynamics which gives the difficulties in the equal coupling case. By using the projection method for the construction of the Fibonacci chain with tile lengths τ, 1 it is not difficult to show that[24]

$$r_n=\alpha n-\frac{1}{\tau}\{n\tau\}\ , \tag{4.3}$$

where $\alpha=1+1/\tau^2$ and $\{x\}$ denotes the fractional part of x. Thus (4.2) contains factors like $\exp(iq\{x\}/\tau)$ where $x=n\tau$. Such factors are periodic in x, with period 1, so can be written as Fourier series[24–26]

$$e^{iy\{x\}}=\sum_m \frac{e^{iy}-1}{i(y-2\pi m)}e^{2\pi imx}\ . \tag{4.4}$$

$S(q,\omega)$ then involves a sum over n, n', k, m, and m', say. The sums over n,n' can be carried out, producing δ functions, which require $m=-m'$ and determine the value of k. As a result,

$$S(q,\omega)=\left[2\sin\frac{q}{2\tau}\right]^2 \times\sum_{m=-\infty}^{\infty}\left[\frac{q}{\tau}-2\pi m\right]^{-2}\delta(\omega-\omega_{\alpha q-2\pi m\tau}) \tag{4.5}$$

is the dynamic structure factor of the Fibonacci chain with equal couplings. Using (4.2) or (4.5) it is straightforward to show that for the special values $q=0$, and $q=2\pi\tau$ the dynamic structure factor is given by

$$S(q=0,\omega)=\delta(\omega)\ , \tag{4.6a}$$

$$S(q=2\pi\tau,\omega)=\delta(\omega-\omega_{2\pi/\tau})\ . \tag{4.6b}$$

Referring to Fig. 5 each curve corresponds to a relationship

$$\omega=\omega_{\alpha q-2\pi\{m\tau\}}=\omega_{\alpha k(q,m)} \tag{4.7}$$

for some m, as given by the separate terms in (4.5). The $m=0$ term has the strongest intensity, for the q values shown in the figure, by virtue of the weight factor $(q/\tau-2\pi m)^{-2}$ in (4.5). Indeed, for $q\to 0$ it gives the full response, and it is the "effective medium" asymptotic eigenstate referred to above. The term "effective medium" is appropriate here, as can be appreciated when it is noticed that in the frequency $\omega_{\alpha q}$ of the $l=0$ term the quantity α is actually the average spacing of sites in the chain. The $m=1,-1$ branches can also be identified readily in the figure and, with a little more difficulty also $m=2,-2$. Thereafter the intensity is very small in the q region covered by the figure. A direct comparison between the results of (4.5) and the generating approach of the previous section, for the special case $J_A=J_B$,was carried out as a check on both methods, and results in agreement to very high precision. The analytic form (4.5) also allows the extraction of rather subtle characteristics of the response, for example hierarchical periodicities: analysis of (4.5) shows that $S(q,\omega)$ is of the form $q^{-2}f(\omega/q^2,\ln q)$ at small ω,q where f is a periodic function of its second argument.

Our main interest in the equal coupling result is however for the interpretation it provides for the general $(J_A\neq J_B)$ case. From Figs. 6–8 as J_B-J_A increases from zero, effective medium behavior persists in the small q limit (with the correct curvature of the dispersion curve) but in general the equal coupling curves develop gaps at their crossing points. These gaps are suggestive of those that occur in weak-coupling approaches to the Bloch energy bands of periodic systems,[27] and in the present case are the gaps in the Cantor set spectrum of the Fibonacci chain. It is therefore of interest to see whether the usual weak coupling approaches (degenerate perturbation theory) can be generalized to provide an explanation of the nature of these figures and in particular the occurrence of arbitrarily many gaps in the horizontally striped fashion exhibited in the figures. This turns out to be possible, and a very brief indication of the procedure will now be given (details will be published elsewhere).

The "unperturbed" starting point is the equal coupling case, for which, according to (4.5) there are unperturbed states, labeled by (q,m) with energy ω as defined in (4.6). The perturbation, proportional to J_B-J_A, has a complicated spatial dependence. Though it can be precisely specified, all we need here is that it is quasiperiodic and can be decomposed into (arbitrary many) Fourier components of which the ith can mix unperturbed states whose $k(q,m)$-labels differ by Q_L, say. The "fundamental" Q_i is $Q_1=2\pi/(1+\tau^2)$ where $(1+\tau^2)$ is the mean spacing of B bonds. So according to degenerate perturbation theory if we had only the $m=0$ branch to consider, dominant splittings should result from the mixing of two $m=0$ states of equal unperturbed energy whose q labels differ by Q_i. This results in the splittings at $q=1.4,0.85$ which are indeed the largest gaps. In general, first order perturbation theory produces a gap when two degenerate states, labeled by q,m and q',m', are linked by a Q_i, i.e., when

$$\omega_{\alpha k(q,m)}=\omega_{\alpha k(q',m')}\ , \tag{4.7a}$$

$$k(q,m)-k(q',m')=Q_i\ . \tag{4.7b}$$

A given Q_i produces the two complete stripes of gaps which open at energies $2J(1\pm\cos\frac{1}{2}\alpha Q_i)$. This explains the striping and the exact positions of gaps in q (for any J_A,J_B) while the gap position in energy is asymptotically correct as $J_A\to J_B$. The perturbation method must, however, fail for the arbitrarily small gaps if J_A-J_B is finite. It nevertheless explains not only all the principal qualitative features, but also gives a quantitative account of most of them.

V. CONCLUSION

We have presented an exact real space renormalization group calculation of the complete wave vector and frequency dependent response function $S(q,\omega)$. Our calculation is based on a recursive evaluation of the generating function $\mathcal{F}$ which involves the change, under a length scale transformation, of the parameters characterizing the physical system (e.g., exchange constants, fields, etc.). Though the pure limit of equal couplings is not trivial due to the quasiperiodicity of the underlying lattice, we were able to obtain an analytic expression for $S(q,\omega)$ for this case.

Our surface plots of the full response $S(q,\omega)$ for the general case of unequal couplings displayed very complicated structure, the main feature being the appearance of striped gaps corresponding to zero response. In addition, we obtained dispersion curves of ω versus q whose features could be understood both qualitatively and quantitatively using ideas of degenerate perturbation theory, in particular the precise location of gaps.

Though we have treated only the fundamental one-dimensional quasicrystal, many of the features obtained and methods used apply also to higher dimensions. In particular, striping and "dispersion curves" should again occur in the support of $S(q,\omega)$. Also, the equal coupling case and its degenerate perturbation theory extension should again be tractable, while the decimation approach,

combined with techniques to be presented elsewhere can give the response function and density of states for certain two-dimensional quasicrystal models. To the best of our knowledge, no experimental work has yet been performed which probes $S(q,\omega)$ (e.g., neutron scattering) and so it is our hope that this present work will stimulate each effort.

ACKNOWLEDGMENTS

One of us (J.A.A.) gratefully acknowledges the support of the Natural Sciences and Engineering Research Council of Canada. The authors are grateful to Dr. J. M. Luck for stimulating discussions on quasicrystals.

[1]B. Simon, Adv. Appl. Math. **3**, 463 (1982).
[2]M. Kohmoto, L. P. Kandanoff, and C. Tang, Phys. Rev. Lett. **50**, 1870 (1986).
[3]S. Ostlund and R. Pandit, Phys. Rev. B **29**, 1394 (1984).
[4]D. Schechtman, I. Blech, D. Gratias, and J. W. Cahn, Phys. Rev. Lett. **53**, 1951 (1984).
[5]D. Levine and P. J. Steinhardt, Phys. Rev. Lett. **26**, 2477 (1984).
[6]M. Kohmoto, B. Sutherland, and C. Tang, Phys. Rev. B **35**, 1020 (1987).
[7]J. M. Luck and Th.M. Nieuwenhuizen, Europhys. Lett. **2**, 257 (1986).
[8]J. M. Luck and D. Petritis, J. Stat. Phys. **42**, 289 (1986).
[9]C. Evangelou, J. Phys. C **20**, L295 (1987).
[10]P. Hawrylak, G. Eliasson, and J. J. Quinn, Phys. Rev. B **36**, 6501 (1987-II).
[11]R. B. Stinchcombe, in *Fractals in Physics,* edited by L. Pietronero and E. Tosatti (Elsevier, New York, 1986).
[12]R. B. Stinchcombe, in *Scaling in Disordered Systems,* edited by R. Pynn and A. Skeltorp (Plenum, New York, 1985).
[13]A.-M.S. Tremblay and B. W. Southern, J. Phys. (Paris) Lett. **44**, L843 (1983).
[14]M.-A. Lemieux and A.-M.S. Tremblay, Phys. Rev. B **36**, 1463 (1987).
[15]A. C. Maggs and R. B. Stinchcombe, J. Phys. A **19**, 398 (1986).
[16]B. W. Southern and P. D. Loly, J. Phys. A **18**, 525 (1985).
[17]J. P. Lu, T. Odagaki, and J. L. Birman, Phys. Rev. B **33**, 4809 (1986).
[18]M. Kantha and R. B. Stinchcombe, J. Phys. A **20**, 495 (1987).
[19]J. A. Ashraff and R. B. Stinchcombe, Phys. Rev. B **37**, 5723 (1988).
[20]R. Merlin, K. Bajema, R. Clarke, F.-T. Juang, and P. K. Bhatacharya, Phys. Rev. Lett. **55**, 1768 (1985).
[21]M. W. C. Dharma-wardana, A. H. MacDonald, D. J. Lockwood, J.-M. Baribeau, and D. C. Houghton, Phys. Rev. Lett. **58**, 1761 (1987).
[22]S. W. Lovesey, *Theory of Neutron Scattering from Condensed Matter* (Oxford University Press, Oxford, 1986), Vols. 1 and 2.
[23]Th. Niemeijer and J. M. J. van Leeuwen, in *Phase Transitions and Critical Phenomena,* edited by C. Domb and M. S. Green (Academic, New York, 1976), Vol. 6.
[24]D. Levine, J. Phys. (Paris) **46**, C8-397 (1985).
[25]The authors are very grateful to Dr. J. M. Luck for pointing this out.
[26]S. Aubry, C. Godreche, and J. M. Luck, Europhys. Lett. **4**, 639 (1987).
[27]R. Peierls, *Quantum Theory of Solids* (Oxford University Press, Oxford, 1965).